Macromolecules

Article

pubs.acs.org/Macromolecules

Polycyclotrimerization of Dinitriles: A New Polymerization Route for the Construction of Soluble Nitrogen-Rich Polytriazines with Hyperbranched Structures and Functional Properties

Carrie Y. K. Chan,[†,‡] Jacky W. Y. Lam,[†,‡] Cathy K. W. Jim,[†,‡] Herman H. Y. Sung,[‡] Ian D. Williams,[‡] and Ben Zhong Tang*[,†,‡,§]

[†]HKUST-Shenzhen Research Institute, No. 9 Yuexing first RD, South Area, Hi-tech Park, Nanshan, Shenzhen 518057, China

[‡]Department of Chemistry, Institute for Advanced Study, Institute of Molecular Functional Materials and Division of Biomedical Engineering, The Hong Kong University of Science and Technology (HKUST), Clear Water Bay, Kowloon, Hong Kong, China

[§]Guangdong Innovative Research Team, SCUT-HKUST Joint Research Laboratory, State Key Laboratory of Luminescent Materials and Devices, South China University of Technology (SCUT), Guangzhou 510640, China

ABSTRACT: A new synthetic route to nitrogen-rich hyperbranched polymers is developed. The polycyclotrimerizations of dinitriles [NC−C_6H_4−$O(CH_2)_4O$−C_6H_4−CN and NC−C_6H_4−$O(CH_2)_4O$−Ar−$O(CH_2)_4O$−C_6H_4−CN Ar = isopropylidenebis(1,4-phenylene), 9,9-fluorenylenebis(1,4-phenylene) and 1,2-diphenylethenylenebis(1,4-phenylene)] catalyzed by trifluoromethanesulfonic acid proceed smoothly in 1,2-dichlorobenzene at room temperature, affording hyperbranched poly(triazine)s with high degree of branching (DB ~63%) in high yields (up to 74.7%). All the polymers are soluble and film-forming. The polymers are thermally and morphologically stable, showing high thermal-degradation and glass-transition temperatures up to 363 and 126.5 °C, respectively. They are optically transparent, allowing almost all visible and IR lights to transmit through. The polymer thin films show high refractive indices (n = 1.7456−1.5857) in a wide spectral region (400−1600 nm) as well as high Abbe numbers (ν_D' up to 187.4) and low optical dispersions (D' down to 0.005). Polymerization of tetraphenylethene-containing dinitrile generates a polymer with aggregation-induced emission characteristic, enabling it to be utilized as a sensitive and selective fluorescent chemosensor for ruthenium(III) ion detection.

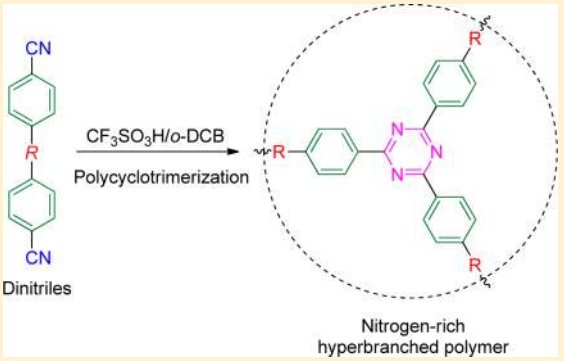

INTRODUCTION

Hyperbranched polymers are a new class of macromolecules and show architectural beauty and multifaceted functionality of dendrimers while enjoying the ease of being prepared by one-pot, single-step procedures.[1] Different synthetic strategies have been developed for the synthesis of hyperbranched polymers[2] and the most commonly used methods are the self-condensation polymerizations of AB_n-type monomers, with A and B being mutually reactive functional groups and $n \geq 2$. These multifunctional monomers, however, are difficult to prepare and suffer from the problem of self-oligomerization during storage.[3] For many years, our group has worked on the construction of functional macromolecules using alkynes as building blocks.[4] With elaborate efforts in the development of functionality-tolerant catalysts and optimization of reaction conditions, we succeeded in the synthesis of a variety of functional hyperbranched polyarylenes through A_2-type polycyclotrimerization (Scheme 1),[5] which can circumvent the synthetic difficulties encountered by the AB_n-type condensation polymerization. For example, the tantalum- or cobalt-catalyzed diyne polycyclotrimerizations can furnish regiorandom hyperbranched polyarylenes with unique optical and photonic properties (**1**, Scheme 1),[6] while the polymerizations of aroylacetylenes or bipropiolates catalyzed by nonmetallic [e.g., piperidine or dimethylformamide (DMF)][7] or transition metals such as Cp*Ru$(PPh_3)_2Cl$[8] generate hyperbranched poly(aroyarylene)s (**2** and **3**) with solely 1,3,5-regiostructures and high degree of branching (DB) in high yields. While all these synthetic polymers possess carbon-based backbones, the backbones of natural polymers or biomacromolecules such as proteins, DNAs, and RNAs contain heteroatoms such as nitrogen and phosphorus. This fact inspires our interest in polymers with carbon-heteroatom backbones, which may show unique properties that are difficult, if not impossible, to access by their counterparts with pure carbon−carbon backbones.

The heterocycles of triazines have become increasingly popular moieties in the design of functional molecules and in the development of specialty materials. Triazines, for example, are very useful in analytical chemistry as complexation agents, in electrochemistry as multistep redox species and in agriculture

Received: October 7, 2013
Revised: November 18, 2013
Published: December 2, 2013

Scheme 1. Construction of Hyperbranched Polyarylenes by Transition Metal-Catalyzed and Metal-Free Diyne Polycyclotrimerizations

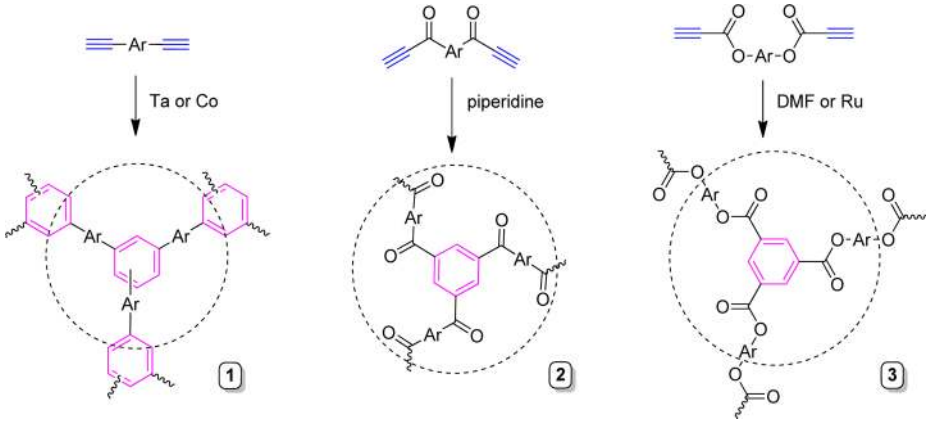

Scheme 2. Polycyclotrimerization of Dinitrites

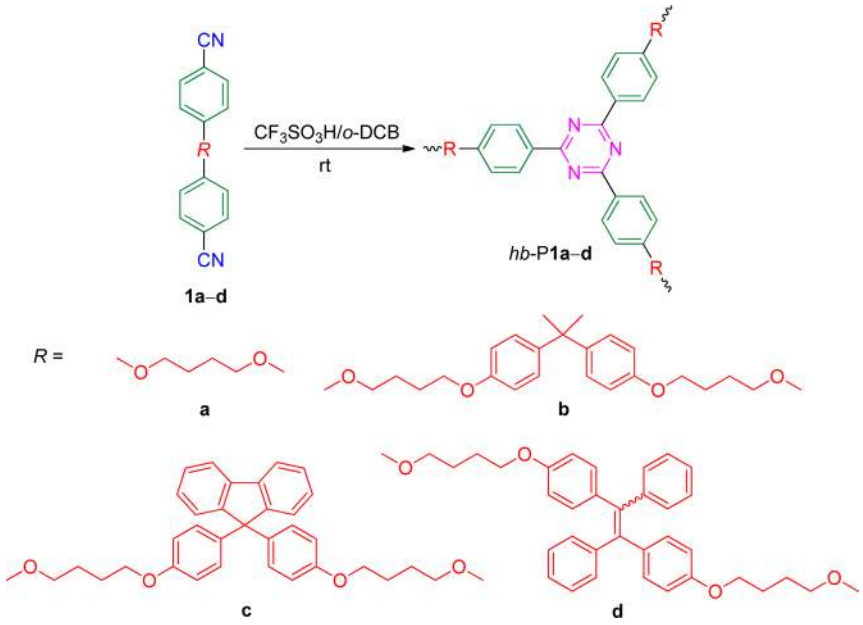

as pesticide and herbicide ingredients.[9] Triazines have found applications in supramolecular chemistry because of their strong tendency for hydrogen bonding and $\pi-\pi$ stacking. For example, self-assembly of triazine-based aggregates with the aid of noncovalent interactions has led to the formation of tubular fibers or three-dimensional porous networks.[10] Triazines also show high affinity or coordination ability to metals.[11] Because of their potential applications in the fields of chemistry, pharmaceutics, and defense and agriculture, organic chemists have synthesized many triazine derivatives by a general method of nitrile cyclotrimerization.[12] This reaction readily occurs under mild conditions with tolerance to a wide variety of functional groups. For example, Norell used trifluoromethanesulfonic acid to catalyze nitrile cyclotrimerization to prepare 1,3,5(*s*)-triazine derivatives.[13] Liu found that organolithium reagent $LiCR_2R'$ (R = $SiMe_3$, R′ = $SiMe_2NMe_2$) catalyzed α-hydrogen-free nitriles to produce 2,4,6-trisubstituted *s*-triazines under mild conditions.[14] Few attempts have also been made to develop this organic reaction for the synthesis of porous polymers. However, all the obtained products are insoluble, which renders them useless from the viewpoint of practical applications.[15] Some soluble polymers and dendrimers containing triazine moieties have been prepared by post-polymerization reactions, but most of them possess inhomogeneous structures because the polymer reactions rarely proceed to completion due to the involved steric effect.

In this work, we explored the possibility of utilizing nitriles as monomers for the construction of nitrogen-rich polymers. By polycyclotrimerization of dinitriles catalyzed by trifluoromethanesulfonic acid, hyperbranched poly(triazine)s with high degree of branching (DB ~63%) are generated (Scheme 2). All the polymers are soluble and thermally and morphologically stable. Their thin films are optically transparent and exhibit high refractive indices with low optical dispersions. Incorporation of tetraphenylethene (TPE), a luminogen with aggregation-induced emission (AIE) characteristics, into the polymer structure generates a polymer with efficient light emission in the aggregated state, which enables it to work as a fluorescent sensor for ruthenium(III) ion detection with high sensitivity and selectivity.

dx.doi.org/10.1021/ma402066k | *Macromolecules* 2013, 46, 9494−9506

EXPERIMENTAL SECTION

Materials and Instruments. Tetrahydrofuran (THF) was distilled from sodium benzophenone ketyl under dry nitrogen immediately prior to use. Solvents such as dichloromethane (DCM), dimethylsulfoxide (DMSO) and dimethylforamide (DMF) and other reagents were purchased from Aldrich and used as received without further purification.

Weight-average molecular weights (M_w) and polydispersities (M_w/M_n) of the polymers were measured by a Waters gel permeation chromatography (GPC) system equipped with a Waters 515 HPLC pump, a set of Waters Styragel columns (HT3, HT4, and HT6 with molecular weight range of 10^2–10^7), a column temperature controller, a Waters 486 wavelength-tunable UV–vis detector, a Waters 2414 differential refractometer and a Waters 2475 fluorescence detector. The polymer solutions were freshly prepared by dissolving in THF (~2 mg/mL) and then filtering through 0.45 μm PTFE syringe-type filters before being injected into the GPC system. THF was served as the mobile phase at a flow rate of 1.0 mL/min. The column temperature and the wavelength of the UV-vis detector were set at 40 °C and 254 nm, respectively. A set of monodispersed polystyrene standards (Waters) covering the molecular weight range of 10^3–10^7 were used for the calibration.

^{1}H and ^{13}C NMR spectra were measured on a Bruker AV 300 spectrometer in deuterated chloroform or DMSO using tetramethylsilane (δ = 0) as internal reference. High resolution mass spectra (HRMS) were measured on a GCT premier CAB048 mass spectrometer operating in MALDI-TOF mode. Infrared (IR) spectra were recorded on a Perkin-Elmer 16 PC FTIR spectrophotometer. UV spectra were measured on a Milton Ray Spectronic 3000 Array spectrophotometer. Photoluminescence (PL) spectra were recorded on a Perkin-Elmer LS 55 spectrofluorometer. Solid-state fluorescence quantum yields (Φ_F) of thin films of the polymers were measured on a calibrated integrating sphere. Thermogravimetric analysis (TGA) was carried on a TA TGA Q5000 under nitrogen at a heating rate of 10 °C/min. The thermal transitions of the polymers were studied by differential scanning calorimetry (DSC) on a TA DSC Q1000 under dry nitrogen at a heating rate of 10 °C/min. The refractive indices (RI or n) of the polymer films were measured on a Metricon PC-2100 prism coupler equipped with a He-Ne laser light source (wavelengths: 403, 473, 632.8, 934, and 1534 nm). The birefringence (Δn) was calculated as the difference between the n_{TE} (in-plane) and n_{TM} (out-of-plane) values.

Preparation of Nanoaggregates. Stock THF solutions of the polymers with a concentration of 10^{-3} M were first prepared. Aliquots of the stock solution were transferred to 10 mL volumetric flasks. After addition of appropriate amounts of THF, water was added dropwise under vigorous stirring to afford 10^{-5} M solutions with different water contents (0–95 vol %). The PL measurements of the diluted solutions were then carried out immediately.

Preparation of Metal Ion Solutions. Aqueous solution of inorganic salts (including sodium chloride, magnesium chloride, iron(II) chloride, iron(III) chloride, cobalt(II) chloride, nickel(II) chloride, copper(II) chloride, zinc chloride, ruthenium(III) chloride, rhodium(III) chloride, palladium chloride, cadmium chloride and lead chloride) of Na^+, Mg^{2+}, Fe^{2+}, Fe^{3+}, Co^{2+}, Ni^{2+}, Cu^{2+}, Zn^{2+}, Ru^{3+}, Rh^{3+}, Pd^+, Cd^{2+} and Pb^{2+} ions were prepared in distilled water with a concentration of 10 mM. The stock solutions were then diluted to desired concentrations with distilled water for further experiments.

Monomer Synthesis. *Synthesis of 4,4′-(1,4-Butylenedioxy)dibenzonitrile (**1a**).* To a 500 mL round-bottomed flask were added 4-hydroxybenzonitrile (**3**, 4.97 g, 41.68 mmol), 1,4-dibromobutane (**4**, 1.6 mL, 13.89 mmol) and K_2CO_3 (9.60 g, 69.47 mmol) in 250 mL of acetone. The reaction mixture was then heated to reflux overnight. After filtration, the solution was concentrated under reduced pressure. The crude product was purified by a silica-gel column chromatography using DCM/hexane (1:2 v/v) as eluent. White solid; yield 91.9%. IR (KBr), υ (cm^{-1}): 2958, 2888, 2221, 1607, 1575, 1509, 1480, 1403, 1302, 1258, 1176, 1058, 1009. ^{1}H NMR (300 MHz, DMSO-d_6), δ (ppm): 7.85 (d, J = 8.7 Hz, 4H), 7.20 (d, J = 8.8 Hz, 4H), 4.23 (m, 4H), 1.98 (m, 4H). ^{13}C NMR (75 MHz, DMSO-d_6), δ (ppm): 162.0, 134.2, 119.2, 115.5, 102.7, 67.6, 25.0. HRMS (MALDI-TOF): m/z 293.1289 [(M+1)$^+$, calcd 293.1212]. Anal. Calcd for $C_{18}H_{16}N_2O_2$: C, 73.95; H, 5.52; N, 9.58; O, 10.95. Found: C, 74.00; H, 5.47; N, 9.66; O, 10.87.

*Synthesis of 4,4′-(Isopropylidene) Bis[(4-bromobutoxy)-benzene] (**6b**) and 9,9-Bis[4-(4-bromobutoxy)phenyl]-fluorene (**6c**).* Compounds **6b** and **6c** were prepared from **5b** (17.52 mmol), **4** (52.56 mmol), and K_2CO_3 (87.61 mmol), and **5c** (11.42 mmol), **4** (34.25 mmol), and K_2CO_3 (57.08 mmol), respectively, using procedures similar to those for **1a**.

*Characterization Data for **6b**.* White solid; yield 60.3%. ^{1}H NMR (300 MHz, $CDCl_3$), δ (ppm): 7.13 (d, J = 8.8 Hz, 4H), 6.78 (d, J = 8.8 Hz, 4H), 3.97 (t, J = 6.4 Hz, 4H), 3.49 (t, J = 6.4 Hz, 4H), 2.08–2.04 (m, 4H), 1.94–1.92 (m, 4H), 1.63 (s, 6H). ^{13}C NMR (75 MHz, $CDCl_3$), δ (ppm): 157.3, 143.9, 128.4, 114.4, 67.4, 42.4, 34.2, 31.7, 30.2, 28.6. HRMS (MALDI-TOF): m/z 498.0855 (M$^+$, calcd 498.0592).

*Characterization Data for **6c**.* White solid; yield 53.3%. ^{1}H NMR (300 MHz, $CDCl_3$), δ (ppm): 7.75 (d, J = 7.6 Hz, 2H), 7.38–7.27 (m, 4H), 7.25–7.24 (m, 2H), 7.10 (d, J = 9.2 Hz, 4H), 6.72 (d, J = 8.8 Hz, 4H), 3.91 (t, J = 6.0 Hz, 4H), 3.45 (t, J = 6.8 Hz, 4H), 2.04–1.99 (m, 4H), 1.90–1.86 (m, 4H). ^{13}C NMR (75 MHz, $CDCl_3$), δ (ppm): 158.2, 152.4, 140.6, 138.8, 129.8, 128.3, 128.0, 126.7, 120.8, 114.7, 67.4, 64.8, 34.2, 33.2, 31.6, 30.1, 28.6. HRMS (MALDI-TOF): m/z 620.0741 [M$^+$, calcd 620.0749].

*Synthesis of 4,4′-[Isopropylidenebis(1,4-phenylene)-dioxybis(1,4-butylene)dioxy]dibenzo-nitrile (**1b**) and 4,4′-[9,9-Fluorenylenebis(1,4-phenylene)dioxybis(1,4-phenylene)-dioxy]dibenzonitrile (**1c**).* Compounds **1b** and **1c** were prepared from **6b** (3.01 mmol), **3** (9.03 mmol), and K_2CO_3 (15.05 mmol), and **6c** (3.22 mmol), **3** (9.67 mmol), and K_2CO_3 (16.12 mmol), respectively, using similar procedures as described above.

*Characterization Data for **1b**.* White solid; yield 54.7%. IR (KBr), υ (cm^{-1}): 2953, 2900, 2872, 2229, 1606, 1576, 1512, 1476, 1405, 1297, 1259, 1178, 1118, 1058, 1006. ^{1}H NMR (300 MHz, DMSO-d_6), δ (ppm): 7.57 (d, J = 8.8 Hz, 4H), 7.13 (d, J = 8.8 Hz, 4H), 6.93 (d, J = 8.8 Hz, 4H), 6.79 (d, J = 9.2 Hz, 4H), 4.08 (t, J = 5.6 Hz, 4H), 4.01 (t, J = 5.6 Hz, 4H), 2.00–1.96 (m, 8H), 1.64 (s, 6H). ^{13}C NMR (75 MHz, DMSO-d_6), δ (ppm): 163.0, 157.4, 143.9, 134.7, 128.4, 120.0, 115.8, 114.4, 104.5, 68.6, 67.8, 42.3, 31.7, 26.6, 26.6. HRMS (MALDI-TOF): m/z 574.3436 (M$^+$, calcd 574.2832). Anal. Calcd for $C_{37}H_{38}N_2O_4$: C, 77.33; H, 6.66; N, 4.87; O, 11.14. Found: C, 77.53; H, 6.70; N, 5.03; O, 10.74.

*Characterization Data for **1c**.* White solid; yield 70.5%. IR (KBr), υ (cm^{-1}): 3063, 2949, 2871, 2219, 1605, 1572, 1508, 1472, 1384, 1303, 1261, 1243, 1176, 1114, 1076, 1044, 1012. ^1H NMR (300 MHz, DMSO-d_6), δ (ppm): 7.75 (d, J = 7.6 Hz, 2H), 7.55 (d, J = 9.6 Hz, 4H), 7.38−7.32 (m, 4H), 7.28−7.24 (m, 2H), 7.10 (d, J = 6.8 Hz, 4H), 6.90 (d, J = 9.2 Hz, 4H), 6.73 (d, J = 6.8 Hz, 4H), 4.05 (t, J = 6.0 Hz, 4H), 3.96 (m, J = 6.0 Hz, 4H), 1.98−1.91 (m, 8H). ^{13}C NMR (75 MHz, DMSO-d_6), δ (ppm): 162.9, 158.3, 152.4, 140.6, 138.9, 134.7, 129.9, 128.4, 128.0, 126.6, 120.9, 120.0, 115.8, 114.7, 104.5, 68.6, 67.8, 64.8, 26.5, 26.5. HRMS (MALDI-TOF): m/z 696.3051 (M^+, calcd 696.2988). Anal. Calcd for $C_{47}H_{40}N_2O_4$: C, 81.01; H, 5.79; N, 4.02; O, 9.18. Found: C, 81.02; H, 5.73; N, 4.13; O, 9.12.

*Synthesis of 4-(4-Bromobutoxy)benzophenone (**8**).* Compound **8** was prepared from **7** (20.18 mmol), **4** (13.45 mmol), and K_2CO_3 (33.63 mmol). The procedures were similar to those of **1a**. White solid; yield 35.0%. ^1H NMR (300 MHz, $CDCl_3$), δ (ppm): 7.82 (d, J = 8.7 Hz, 2H), 7.74 (d, J = 8.3 Hz, 2H), 7.58−7.49 (m, 1H), 7.46−7.43 (m, 2H), 6.94 (d, J = 8.8 Hz, 2H), 4.11−4.05 (m, 2H), 3.51−3.47 (m, 2H), 2.10−1.95 (m, 4H). ^{13}C NMR (75 MHz, $CDCl_3$), δ (ppm): 196.1, 163.1, 138.8, 133.2, 132.5, 130.7, 130.3, 128.8, 114.6, 67.7, 33.9, 29.9, 28.3. HRMS (MALDI-TOF): m/z 333.0110 [$(M+1)^+$, calcd 333.0412].

*Synthesis of 1,2-Bis[4-(4-bromobutoxy)phenyl]-1,2-diphenylethene (**9**).* In a two-necked flask equipped with a magnetic stirrer were added **8** (1.5g, 4.5 mmol), zinc powder (0.59 g, 9.0 mmol), and 40 mL of THF. After the mixture was cooled to −78 °C, $TiCl_4$ (0.5 mL, 4.5 mmol) was slowly added by a syringe. The mixture was warmed to room temperature, stirred for 0.5 h, and then heated to reflux for overnight. After being cooled to room temperature, the reaction mixture was quenched with aqueous hydrochloric acid solution and extracted with dichloromethane. The organic layer was collected and concentrated. The crude product was purified by silica-gel column chromatography using hexane as eluent to give a yellow liquid in 82.6% yield (1.18 g). ^1H NMR (300 MHz, $CDCl_3$), δ (ppm): 7.10−7.03 (m, 10H), 6.96−6.89 (m, 4H), 6.62 (t, J = 8.8 Hz, 4H), 3.95−3.89 (m, 4H), 3.51−3.45 (m, 4H), 2.10−2.02 (m, 4H), 1.99−1.87 (m, 4H). ^{13}C NMR (75 MHz, $CDCl_3$), δ (ppm): 157.9, 144.9, 144.9, 140.3, 137.2, 137.1, 133.2, 132.1, 128.3, 128.2, 126.9, 114.3, 114.2, 67.3, 67.2, 34.2, 30.2, 28.6. HRMS (MALDI-TOF): m/z 634.0459 (M^+, calcd 634.0905).

*Synthesis of 4,4′-[1,2-Diphenylethenylenebis(1,4-phenylene)dioxybis(1,4-butylene)dioxy] Dibenzonitrile (**1d**).* Monomer **1d** was prepared from **9** (1.39 mmol), **3** (4.16 mmol), and K_2CO_3 (6.94 mmol) using procedures similar to those for **1a**. Yellow liquid; yield 94.8%. IR (KBr), υ (cm^{-1}): 3050, 2943, 2873, 2223, 1605, 1573, 1508, 1471, 1390, 1302, 1242, 1171, 1111, 1044, 1013. ^1H NMR (300 MHz, DMSO-d_6), δ (ppm): 7.57 (d, J = 8.8 Hz, 4H), 7.10−7.02 (m, 10H), 6.96−6.89 (m, 8H), 6.62 (t, J = 9.1 Hz, 4H), 4.09−4.04 (m, 4H), 3.98−3.93 (m, 4H), 2.00−1.92 (m, 8H). ^{13}C NMR (75 MHz, DMSO-d_6), δ (ppm): 162.9, 157.9, 145.0, 144.8, 140.3, 137.2, 137.1, 134.7, 133.2, 132.1, 128.3, 128.2, 126.9, 120.0, 115.8, 114.2, 114.2, 104.5, 68.6, 67.8, 26.5. HRMS (MALDI-TOF): m/z 710.2960 (M^+, calcd 710.3145). Anal. Calcd for $C_{48}H_{42}N_2O_4$: C, 81.10; H, 5.96; N, 3.94; O, 9.00. Found: C, 81.10; H, 6.03; N, 4.03; O, 8.84.

Polymer Synthesis. All the polymerization reactions and manipulations were performed under nitrogen atmosphere using the standard Schlenk technique in a vacuum line system or an inert atmosphere glovebox (Vacuum Atmosphere). Purification of the polymers, on the other hand, was done in an open atmosphere. The polycyclotrimerization reactions were catalyzed by trifluoromethanesulfonic acid (CF_3SO_3H) in *o*-dichlorobenzene (*o*-DCB). A typical experimental procedure for the polymerization of **1a** is given in the following as an example.

In a 20 mL test tube equipped with a magnetic stirrer were placed **1a** (0.25 mmol) and CF_3SO_3H (1 mmol) in 2 mL *o*-DCB. The mixture solution was stirred at room temperature for 1 h. Afterward, the polymerization was terminated by pouring the reaction mixture into 300 mL of methanol/hexane solvent mixture (1:5 v/v) via cotton filter. The precipitates were filtered by a Gooch crucible, washed with methanol and hexane for three times, and finally dried in vacuum overnight at room temperature.

Characterization Data for *hb*-P1a. Pale yellow solid; yield 74.7% (Table 4, no. 2). M_w 15 660; M_w/M_n 2.17 (GPC, polystyrene calibration). IR (KBr), υ (cm^{-1}): 2940, 2867, 1607, 1584, 1505, 1419, 1367, 1249, 1173, 1146, 1109. ^1H NMR (300 MHz, DMSO-d_6), δ (ppm): 8.67, 7.90, 7.85, 7.19, 7.07, 6.91, 6.88, 4.18, 3.61, 3.38, 3.27, 1.79. ^{13}C NMR (75 MHz, DMSO-d_6), δ (ppm): 170.8, 170.6, 170.0, 165.9, 165.7, 162.4, 161.8, 160.8, 160.0, 134.1, 130.7, 130.4, 129.0, 128.9, 127.9, 126.7, 126.5, 125.4, 115.6, 114.7, 113.8, 71.5, 69.7, 67.4, 26.0, 25.6, 25.3.

***hb*-P1b:** Yellow solid; yield 41.9% (Table 4, no. 5). M_w 8 490; M_w/M_n 1.54 (GPC, polystyrene calibration). IR (KBr), υ (cm^{-1}): 2950, 2868, 1606, 1584, 1507, 1419, 1368, 1246, 1172, 1145, 1029. ^1H NMR (300 MHz, DMSO-d_6), δ (ppm): 8.69, 8.63, 8.60, 8.34, 7.86, 7.74, 7.69, 7.30, 7.10, 7.04, 6.94, 6.90, 6.77, 4.19, 4.06, 3.88, 1.96. ^{13}C NMR (75 MHz, DMSO-d_6), δ (ppm): 171.1, 170.8, 170.0, 166.9, 162.3, 158.5, 156.2, 150.0, 144.0, 137.5, 133.8, 131.1, 130.3, 129.2, 128.9, 128.5, 128.1, 128.0, 127.2, 126.7, 126.3, 125.1, 120.2, 115.2, 114.2, 113.8, 113.6, 69.8, 67.3, 66.9, 26.0, 25.4.

***hb*-P1c:** Pale yellow solid; yield 60.4% (Table 4, no. 8). M_w 8 770; M_w/M_n 1.80 (GPC, polystyrene calibration). IR (KBr), υ (cm^{-1}): 3037, 2942, 2871, 1606, 1584, 1507, 1473, 1447, 1419, 1369, 1247, 1174, 1147, 1112, 1030. ^1H NMR (300 MHz, DMSO-d_6), δ (ppm): 8.66, 7.73, 7.65, 7.60, 7.55, 7.52, 7.36, 7.09, 7.02, 6.99, 6.93, 6.91, 6.87, 6.83, 6.81, 6.74, 6.71, 3.97, 3.95, 3.47, 3.41, 3.37, 3.33, 1.93. ^{13}C NMR (75 MHz, DMSO-d_6), δ (ppm): 171.5, 162.7, 161.4, 153.9, 141.2, 139.8, 133.7, 131.4, 130.2, 130.1, 130.0, 129.9, 128.4, 128.0, 127.9, 127.4, 126.7, 126.2, 120.8, 120.5, 115.8, 115.5, 115.3, 115.2, 115.0, 114.8, 71.3, 68.3, 68.0, 66.5, 27.2, 26.7.

***hb*-P1d:** Pale yellow solid; yield 65.6% (Table 4, no. 11). M_w 16 640; M_w/M_n 2.23 (GPC, polystyrene calibration). IR (KBr), υ (cm^{-1}): 3051, 2944, 2872, 2224, 1584, 1507, 1472, 1419, 1369, 1301, 1243, 1172, 1146, 1111, 1015. ^1H NMR (300 MHz, DMSO-d_6), δ (ppm): 8.70, 8.68, 7.57, 7.54, 7.08, 7.04, 7.01, 6.95, 6.92, 6.89, 6.66, 6.63, 6.60, 4.13, 4.04, 4.02, 3.98, 3.96, 3.94, 1.98, 1.94. ^{13}C NMR (75 MHz, DMSO-d_6), δ (ppm): 171.4, 163.2, 162.9, 158.2, 158.0, 145.0, 144.9, 140.7, 140.1, 139.9, 137.1, 137.0, 135.0, 134.6, 134.0, 133.3, 132.0, 131.4, 129.7, 128.3, 126.8, 126.7, 119.9, 118.1, 115.8, 115.0, 114.2, 114.2, 106.0, 104.5, 68.6, 68.4, 67.9, 67.7, 26.7, 26.5, 26.5.

Model Reaction. 4-Ethoxybenzonitrile (**10**) was prepared from etherization of **3** (40.19 mmol) with 1-bromoethane (26.8 mmol) in the presence of K_2CO_3 (67.0 mmol). The procedures

dx.doi.org/10.1021/ma402066k | *Macromolecules* 2013, 46, 9494−9506

Scheme 3. Synthesis of Dinitriles 1a–d

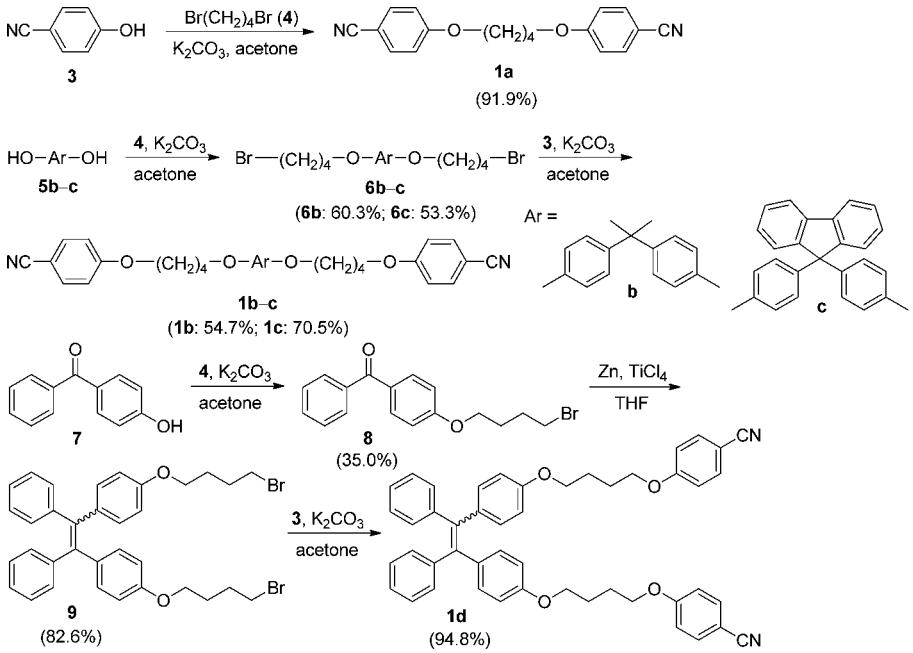

were similar to those for **1a**. White solid; yield 100%. ^{1}H NMR (300 MHz, $CDCl_3$), δ (ppm): 7.57 (d, J = 8.6 Hz, 2H), 6.93 (d, J = 8.7 Hz, 2H), 4.11–4.04 (m, 2H), 1.44 (t, J = 7.0 Hz, 3H). ^{13}C NMR (75 MHz, $CDCl_3$), δ (ppm): 162.9, 134.6, 120.0, 115.8, 104.4, 64.6, 15.2. HRMS (MALDI-TOF): m/z 148.0762 [$(M+1)^+$, calcd 148.0684].

*Synthesis of Tris(4-ethoxyphenyl)triazine (**2**).* To a vigorously stirred solution of CF_3SO_3H (2 mL, 8.15 mmol) in dry chloroform (5 mL) was added **10** (0.6 g, 4.08 mmol) dropwise in dry chloroform (20 mL) at 0 °C and under a stream of nitrogen. After 2 h, the mixture was warmed to room temperature and stirred for additional 24 h. The reaction mixture was then poured into water containing a small amount of ammonium hydroxide. The organic layer was washed three times with water and then dried over magnesium sulfate. After filtration and solvent evaporation, the crude product was purified by silica-gel column chromatography using hexane/DCM mixture (4:1 v/v) as eluent. White solid; yield 75.9%. ^{1}H NMR (300 MHz, DMSO-d_6), δ (ppm): 8.73 (d, J = 8.8 Hz, 6H), 7.24 (d, J = 8.8 Hz, 6H), 4.27 (m, 6H), 1.49 (t, J = 6.9 Hz, 9H). ^{13}C NMR (75 MHz, DMSO-d_6), δ (ppm): 170.1, 162.4, 130.5, 127.8, 114.6, 63.5, 14.6. HRMS (MALDI-TOF): m/z 442.2203 [$(M+1)^+$, calcd 442.2052]. Anal. Calcd for $C_{27}H_{27}N_3O_3$: C, 73.45; H, 6.16; N, 9.52; O, 10.87. Found: C, 73.46; H, 6.11; N, 9.47; O, 10.96. Crystallographic data for **2** has been deposited with the Cambridge Crystallographic Data Centre as supplementary publication no. CCDC 960230.

RESULTS AND DISCUSSION

Monomer Synthesis. We adopted an A_2-type polycyclotrimerization approach to prepare nitrogen-rich macromolecules using dinitriles as building blocks. We designed and prepared monomers **1a–d** according to the synthetic procedures shown in Scheme 3. While dinitrile **1a** was prepared by etherization of 4-hydroxybenzonitrile (**3**) with 1,4-dibromobutane (**4**), compounds **1b** and **1c** were obtained by nucleophilic substitution of **4** with respective dihydroxyarenes followed by etherization of resulting intermediates with **3**.

Table 1. Catalytic Effect of Different Protonic Acids on the Polycyclotrimerization of 1a[a]

entry	catalyst	yield (%)	M_w[b]	M_w/M_n[b]
1	CF_3CO_2H	0		
2	$MeSO_3H$	0		
3	$ClSO_3H$	trace	2000	1.9
4	CF_3SO_3H	62.3	14 500	2.2

[a]Carried out in *o*-DCB under nitrogen for 30 min. [**1a**] = 0.125 M; [catalyst] = 0.5 M. [b]Determined by GPC in THF on the basis of a polystyrene calibration.

Table 2. Solvent Effect on the Polycyclotrimerization of 1a[a]

entry	solvent	yield (%)	M_w[b]	M_w/M_n[b]
1	DCE	trace		
2	*o*-xylene	trace		
3	DCM	22.6	7900[c]	1.6
4	$CHCl_3$	50.5	15 900[c]	2.6
5[d]	*o*-DCB	62.3	14 500	2.2

[a]Carried out under nitrogen for 30 min. [**1a**] = 0.125 M; [CF_3SO_3H] = 0.5 M. Abbreviation: DCE = 1,2-dichloroethane, DCM = dichloromethane, and *o*-DCB = 1,2-dichlorobenzene. [b]Determined by GPC in THF on the basis of a polystyrene calibration. [c]Soluble fraction. [d]Data taken from Table 1, no. 4.

Compound **9** was synthesized by reaction of 4-hydroxybenzophenone (**7**) with **4** followed by McMurry coupling of the resulting product (**8**) catalyzed by $TiCl_4$/Zn in THF. Its etherization with **3** finally gave the desirable product **1d**. One noticeable structural feature of all the monomers is that they possess long alkyl chains for the purpose of endowing the resulting polymers with good processability. All the compounds including the intermediates were characterized by spectroscopic techniques, from which satisfactory analysis data corresponding to their expected molecular structures were obtained.

Polymerization. After obtaining the dinitrile monomers, we systematically investigated their polymerization behaviors. Lewis and protonic acids are the most commonly used catalysts

dx.doi.org/10.1021/ma402066k | Macromolecules 2013, 46, 9494–9506

Table 3. Effects of Monomer and Catalyst Concentrations on the Polymerization of 1a[a]

entry	[1a] (M)	[CF_3SO_3H] (M)	[CF_3SO_3H]/[1a]	yield (%)	M_w[b]	M_w/M_n[b]
1	0.100	0.40	4	43.5	6600	1.5
2	0.125	0.25	2	gel		
3	0.125	0.75	6	27.4	7000	1.5
4[c]	0.125	0.50	4	62.3	14 500	2.2
5	0.150	0.60	4	gel		
6	0.175	0.70	4	gel		
7[d]	0.125	11.30	10	trace		

[a]Carried out under nitrogen in *o*-DCB at room temperature for 30 min. [b]Determined by GPC in THF on the basis of a polystyrene calibration. [c]Data taken from Table 1, no. 4. [d]No *o*-DCB was added.

Table 4. Polymerization of 1a–d[a]

entry	monomer	time (h)	yield (%)	M_w[b]	M_w/M_n[b]
1[c]	**1a**	0.5	62.3	14 500	2.2
2		1.0	74.7	15 700	2.2
3		2.0	63.3	12 700	2.1
4	**1b**	2.0	trace		
5		4.0	41.9	8 500	1.5
6	**1c**	2.0	trace		
7		4.0	60.4	8 800	1.8
8		6.0	gel		
9	**1d**	1.0	18.3	4 600	1.2
10		2.0	65.6	16 600	2.2

[a]Carried out under nitrogen in *o*-DCB at room temperature. [monomer] = 0.125 M, [CF_3SO_3H] = 0.5 M (nos. 1–3 and 10) or [monomer] = 0.25 M, [CF_3SO_3H] = 1.0 M (nos. 4–9 and 11). [b]Determined by GPC in THF on the basis of a polystyrene calibration. [c]Data taken from Table 1, no. 4.

for the cyclotrimerization of aromatic nitriles.[12] Since the former ones generally consists of metallic species, they are harmful to the environment and also the materials properties of the resulting polymers if they are not completely removed. We are interested in exploring new metal-free polymerization routes and thus focused our search on a variety of protonic acids. As shown in Table 1, polymerization of **1a** catalyzed by CF_3CO_2H and $MeSO_3H$ in *o*-DCB gives no polymeric products. Attempt to use a stronger acid of $ClSO_3H$ afforded only a trace amount of product with a low molecular weight. Delightfully, when an even stronger acid of CF_3SO_3H was employed, a polymer with a weight-average molecular weight of 14 500 was obtained in a reasonable high yield (62.3%). It seems that the catalytic activity of the protonic acids correlates with their strength. Among the tested acids, CF_3SO_3H is the strongest one with the largest acid dissociation constant, which helps initiate the polymerization reaction.

To further search for optimal reaction conditions, we then examined the solvent effect on the dinitrile polycyclotrimerization (Table 2). Reaction of **1a** catalyzed by CF_3SO_3H in DCE and *o*-xylene generates only a trace amount of polymeric products. Although polymers are isolated in much higher yields in DCM and $CHCl_3$, they are only partially soluble. Completely soluble polymers, however, are obtained in *o*-DCB, enabling us to investigate their structures and properties by wet spectroscopic methods.

Table 5. Summary of Crystal Data and Intensity Collection Parameters for 2 (CCDC 960230)

	model compound **2**
empirical formula	$C_{26.88}H_{26.88}N_3O_{3.12}$
formula weight	441.87
crystal dimensions, mm	0.22 × 0.19 × 0.07
crystal system	monoclinic
space group	*P*2(1)/*c*
a, Å	8.0066(4)
b, Å	17.2584(9)
c, Å	17.1625(7)
α, deg	90
β, deg	100.565(5)
γ, deg	90
V, Å^3	2331.33(19)
Z	4
D_{calcd}, gcm^3	1.259
F_{000}	936
temp, (K)	173.0
Rradation (λ), Å	1.5418
μ (Mo Kα) mm^{-1}	0.669
$2\theta_{max}$, deg (completeness)	66.50 (95.9%)
no. of collected reflns.	7318
no. of unique reflns. (R_{int})	4044 (0.0257)
data/restraints/parameters	4044/0/309
R_1, wR_2 [obs I> 2σ (I)]	0.0495, 0.1275
R_1, wR_2 (all data)	0.0588, 0.1340
residual peak/hole e. Å^{-3}	0.324/−0.166
transmission ratio	1.00/0.77
goodness-of-fit on F^2	1.040

Scheme 4. Synthetic Route to the Model Compound

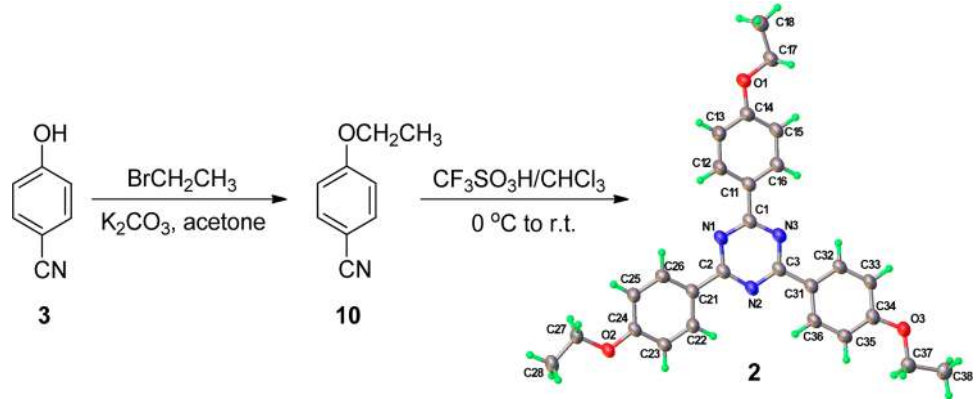

dx.doi.org/10.1021/ma402066k | *Macromolecules* 2013, 46, 9494–9506

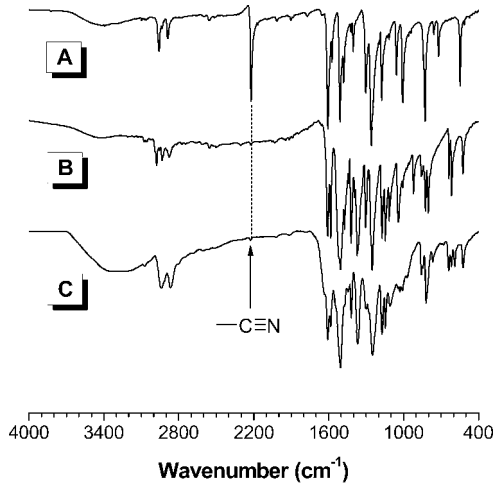

Figure 1. IR spectra of (A) monomer **1a**, (B) model compound **2** and (C) polymer *hb*-P**1a**.

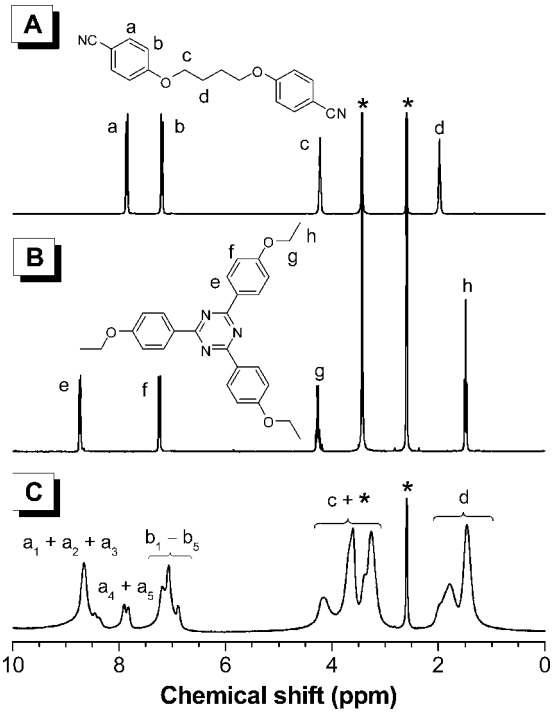

Figure 2. ^{1}H NMR spectra of (A) monomer **1a**, (B) model compound **2** and (C) polymer *hb*-P**1a** in DMSO-d_6. The solvent peaks were marked with asterisks.

Table 3 shows the effects of monomer and acid concentrations on the polycyclotrimerization of **1a** in *o*-DCB. The polymerization conducted at 0.1 M of **1a** and 0.4 M of CF_3SO_3H furnishes a polymer with an M_w value of 6600 in 43.5% yield. Lowering the monomer molar ratio from 4 to 2 gives an insoluble gel, while increasing the value to 6 has lowered the yield (Table 3, no. 2 and 3). Raising both the concentrations of **1a** and CF_3SO_3H, while keeping their molar ratio unchanged, results in improved results or insoluble gels (Table 3, nos. 4–6). Thus, precise control on both the parameters, especially the monomer concentration, is important for the occurrence of smooth polymerization. The polymerization does not proceed in the absence of *o*-DCB. The time course on the polymerization was also followed, and the results are summarized in Table 4, nos. 1–3. Both the yield and molecular weight are enhanced by lengthening the reaction time from 30 min to 1 h. However, no further improvement was observed when the reaction time was increased to 2 h.

Polycyclotrimerizations of other dinitriles **1b–d** are carried out under the conditions shown in Table 4, nos. 4–10. Results show that higher monomer and acid concentrations as well as longer reaction time are required to obtain satisfactory polymerization results. For example, hyperbranched polymers *hb*-P**1b** and *hb*-P**1c** are obtained in moderate yields of 41.9 and 60.4% by acid-catalyzed polycyclotrimerizations of **1b** and **1c**, respectively, in *o*-DCB for 4 h. Under the same conditions, polymerization of **1d** for 2 h generates *hb*-P**1d** in 65.6% yield with a higher molecular weight of 16 600. It should be pointed out that the molecular weights are probably considerably underestimated because of the hyperbranched nature of the polymers.[16] Our previous investigations reveal that the underestimation can be very large and up to 7-fold.[17] The absolute molecular weights of the present polymers should be much higher than the relative values estimated from the GPC analysis.

Model Reaction. To verify that the dinitrile monomers have indeed underwent polycyclotrimerization in the presence of acid and gain insights into the structures of *hb*-P**1a–d**, we conducted a model reaction and prepared **2** as a model compound from **10** (Scheme 4). Compound **10** was prepared by etherization of **3** with 1-bromoethane in the presence of K_2CO_3. Its cyclotrimerization was catalyzed by CF_3SO_3H in dry chloroform, affording tris(4-ethoxyphenyl)triazine (**2**) in a quantitative yield. The structure of the model compound was characterized by standard spectroscopic techniques with satisfactory results (see Experimental Section for details). Compound **2** was further confirmed by single crystal X-ray diffraction, and its crystal data are summarized in Table 5.

Structural Characterization. The polymers were characterized by spectroscopic methods with satisfactory results. An example of the IR spectrum of *hb*-P**1a** is given in Figure 1; for comparison, the spectra of its monomer and model compound **2** are also given in the same figure. The C≡N stretching vibration of **1a** occurs at 2221 cm^{-1}, which disappears completely in the spectrum of *hb*-P**1a**. This indicates that almost all the C≡N bonds of **1a** have been transformed to the triazine units in *hb*-P**1a** by the polymerization reaction. The spectrum of *hb*-P**1a** largely resembles to that of **2** because the former is basically constructed from the latter.

The ^{1}H NMR spectra of *hb*-P**1a** and its monomer **1a** as well as the model compound are shown in Figure 2. By comparison with the spectra of **1a** and **2**, the resonance peaks in the spectrum of *hb*-P**1a** can be readily assigned (Chart 1). For example, the peak at δ 8.67 in *hb*-P**1a** is due to the resonances of the phenyl protons ortho to the triazine rings of its dendritic, linear and terminal units. Some nitrile groups remain unreacted and exist as end groups in the polymer, as suggested by the appearance of a doublet peak at δ ~7.88. On the other hand, the ^{13}C NMR spectrum of *hb*-P**1a** shows no resonance peak of nitrile carbon of **1a** at δ 102.7 (Figure 3). New peaks corresponding to the absorptions of the triazine carbons are observed at δ 170.8, 170.6, and 169.9 due to the conversion of the nitrile groups of **1a** to triazine rings of *hb*-P**1a**.

Degree of Branching. An important parameter for a hyperbranched polymer is its DB value,[18] which is usually determined by ^{1}H NMR spectral analysis. As shown in Chart 1, there are three structural components found in *hb*-P**1a**:

dx.doi.org/10.1021/ma402066k | *Macromolecules* 2013, 46, 9494–9506

Chart 1. Chemical Structure of the Hyperbranched Polymer *hb*-P1a

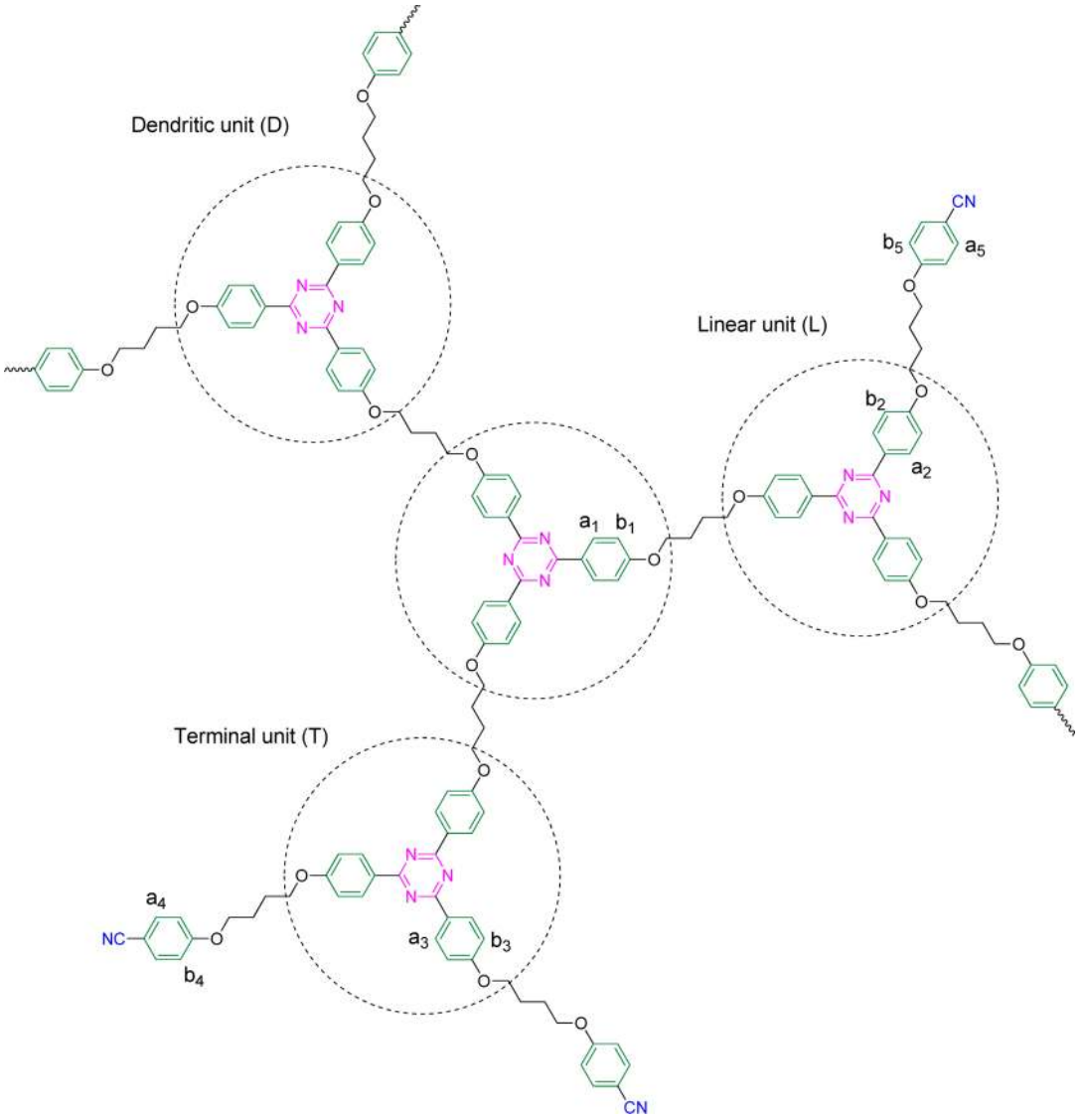

dendritic (D), linear (L) and terminal (T) units. Comparing the ^{1}H NMR spectrum of *hb*-P**1a** with those of its monomer and the model compound, the below relationships between the contents or fractions (f) of the structural units can be established.

$$\frac{6f_D + 6f_L + 6f_T}{2f_L + 4f_T} = \frac{3f_D + 3f_L + 3f_T}{f_L + 2f_T} = \frac{A_{a1-a3}}{A_{a4-a5}} \quad (1)$$

$$f_D + f_L + f_T = 1 \quad (2)$$

where A_{a1-a3} and A_{a4-a5} represent the integrals of the areas of resonance peaks (a_1–a_3) and (a_4–a_5), respectively, as labeled in Chart 1. The values can be determined from the ^{1}H NMR data, from which the following equation is deduced:

$$\frac{3}{f_L + 2f_T} = \frac{1}{0.481} \quad (3)$$

By combining eq 2 and 3, eq 4 can be obtained:

$$f_L + 2f_T = 1.443 \quad (4)$$

The doublet peak at around δ 7.88 corresponds to the resonances of the phenyl protons ortho to the nitrile groups in the L and T units of the polymer. The amount of these protons in the L unit is ~2.86-fold lower than that in the T unit. Since there are four such protons in the T unit but only two in the L unit, eq 5 thus holds:

$$\frac{f}{2f_T} = \frac{1}{2.858} \quad (5)$$

From the above equations, f_L is then calculated to be:

$$f_L = 0.374 \quad (6)$$

DB of a hyperbranched polymer is defined as the ratio of the number of its dendritic and terminal units to its total structural units.[19] According to this definition, DB of *hb*-P**1a** is expressed as follows:

$$DB = \frac{f_D + f_T}{f_D + f_L + f_T} \quad (7)$$

Incorporating eq 2 and 6 into eq 7 gives the DB value of *hb*-P**1a**:

dx.doi.org/10.1021/ma402066k | *Macromolecules* 2013, 46, 9494–9506

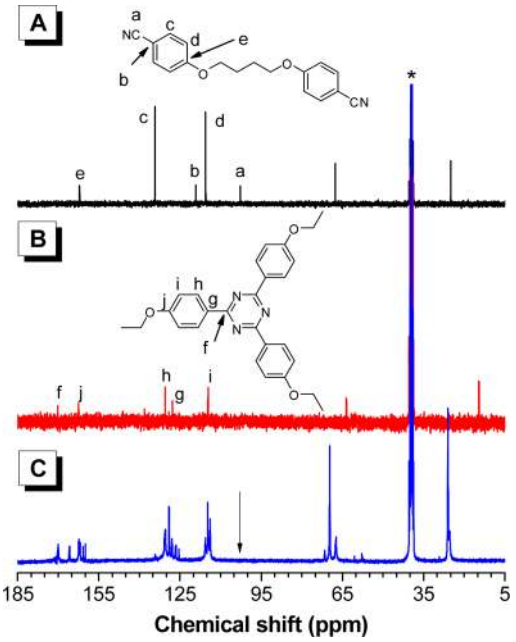

Figure 3. ^{13}C NMR spectra of (A) monomer **1a**, (B) model compound **2**, and (C) polymer *hb*-P**1a** in DMSO-d_6. The solvent peaks were marked with asterisks.

Table 6. Solubility of the Hyperbranched Polymers[a]

	hb-P**1a**	*hb*-P**1b**	*hb*-P**1c**	*hb*-P**1d**
hexane	×	×	×	×
toluene	×	×	×	×
dimethyl ether	×	×	×	×
dioxane	√	√	√	√
dichloromethane	Δ	Δ	Δ	Δ
chloroform	Δ	√	√	√
tetrahydrofuran	√	√	√	√
ethyl acetate	×	×	×	×
acetone	×	×	×	×
acetonitrile	×	×	×	×
ethanol	×	×	×	×
methanol	×	×	×	×
dimethylformamide	√	√	√	√
dimethylsulfoxide	√	√	√	√

[a]Solubility tested in common organic solvents. Abbreviation: √ = completely soluble, Δ = partially soluble, × = insoluble.

$$DB = 1 - f_L = 0.626 \quad (8)$$

This value is higher than those of the "conventional" hyperbranched polymers with the most probable value of ~0.5.[18,20]

Solubility and Thermal Stability. Table 6 shows the solubility of *hb*-P**1a**−**d**. All the polymers are completely soluble in some common organic solvents, such as dioxane, THF, DMF, and DMSO, but partially soluble in DCM and chloroform. Their solubility in nonpolar (e.g., hexane, toluene and dimethyl ether), polar protonic (e.g., ethanol and methanol), and some of the polar aprotic (e.g., ethyl acetate, acetone and acetonitrile) solvents are generally low. They can be readily fabricated into tough solid films by spin-coating or solution-casting process.

In general, optical materials manufactured by the injection molding process require a glass-transition temperature (T_g) of above 100 °C or preferably even 120 °C. On the other hand, the stability of the materials is of primary concern for the high-temperature process. The thermal properties of the hyperbranched polytriazines are evaluated by TGA. As shown in Figure 4A, the temperatures for 5% weight loss or the degradation temperatures (T_d) of the *hb*-P**1a**−**d** are all above 220 °C. Among them, *hb*-P**1d** exhibits the highest T_d (363 °C) because of its higher aromatic content. We also studied the thermal transitions of the polymers by DSC measurement and detected glass-transition temperatures (T_g) at 87.2−126.5 °C in the second heating scan. The above results demonstrate that *hb*-P**1a**−**d** enjoy both high thermal and morphological stabilities, which satisfy the need for optical applications.

Optical Properties. The UV spectra of *hb*-P**1a**−**d** in THF solutions are depicted in Figure 5. All the polymers exhibit an absorption maximum peak at 310 nm. They absorb little lights in the visible spectral region and allow all the lights at wavelengths longer than 400 nm to transmit through. Such a good optical transparency is due to the presence of electronically saturated butyl chains in their molecular structures, which weakens the electronic communication between the aromatic rings and hence decreases the extent of electronic conjugation. The high optical clarity of *hb*-P**1a**−**d** make them promising for photonic applications.

Our group is interested in studying a novel class of luminogens with aggregation-induced emission (AIE) characteristics.[21,22] Unlike conventional luminophores, in which molecular aggregation promotes the formation of detrimental species such as excimers and exciplexes and hence leads to undesired nonradiative transitions,[23] the light emission of AIE luminogens is enhanced by aggregate formation. Development of AIE materials is thus of academic value as well as technological implication. Many studies on small AIE molecules with twisted structures have been performed. In order to improve the processability of low molecular weight compounds, we extent our AIE research to polymeric system.[24] We incorporated TPE into the structure of hyperbranched polytriazine and generated *hb*-P**1d** carrying AIE luminogenic units. Upon photoexcitation, only noisy PL signals with no discernible peak maximum are observed in the PL spectrum of *hb*-P**1d** in dilute THF solution (10 μM; Figure 6). Gradual addition of water, a nonsolvent for *hb*-P**1d**, into its THF solution has progressively enhanced its light emission without large change in the spectral pattern. To have a quantitative picture on the emission enhancement process, we measured its fluorescence quantum yield in both solution ($\Phi_{F,S}$) and solid ($\Phi_{F,F}$) states. The $\Phi_{F,S}$ determined using 9,10-diphenylanthracene (Φ_F = 90% in cyclohexane) as standard is 1.8%. The $\Phi_{F,F}$ value in the amorphous state measured by a calibrated integrating sphere is much higher and equal to 16.9%. Clearly, *hb*-P**1d** is AIE-active.

Light Refraction. Polymeric materials with high refractive indices (RI or n) have attracted considerable interest because of their lightweight, impact resistance, processability, and dying ability compared to inorganic glasses,[25] which make them suitable for high-technological applications as optical materials, such as lenses, prisms, and waveguides. Our hyperbranched polymers possess polarizable aromatic rings and may show high RI values. Indeed, as shown in Figure 7, *hb*-P**1a** displays high refractivities (n = 1.7296−1.6046) in a wide spectral region (400−1600 nm). *hb*-P**1b**−**d** also exhibit high refractive indexes of 1.6607−1.5857, 1.7087−1.6031, and 1.7456−1.6229, respectively, in the same spectral region. The n values of the

dx.doi.org/10.1021/ma402066k | *Macromolecules* 2013, 46, 9494−9506

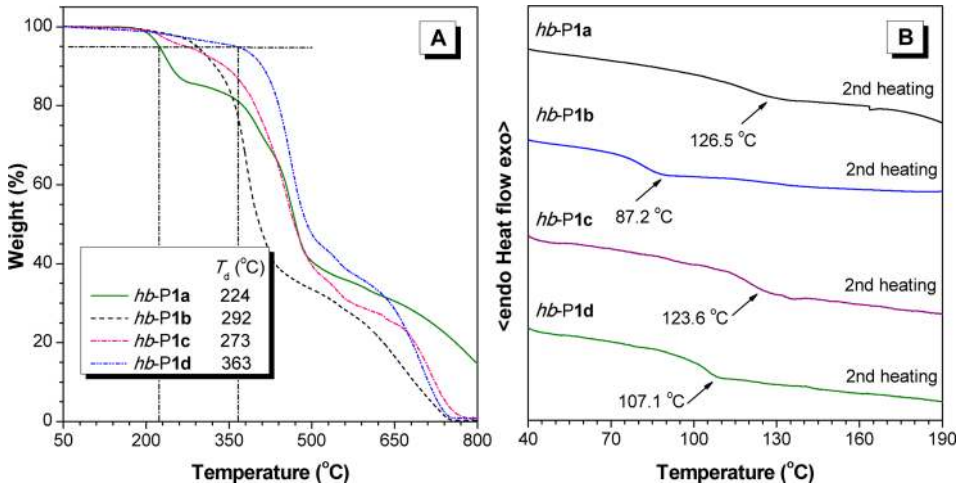

Figure 4. (A) TGA and (B) DSC thermograms of *hb*-P**1a**–**d** recorded under nitrogen at a heating rate of 10 °C/min.

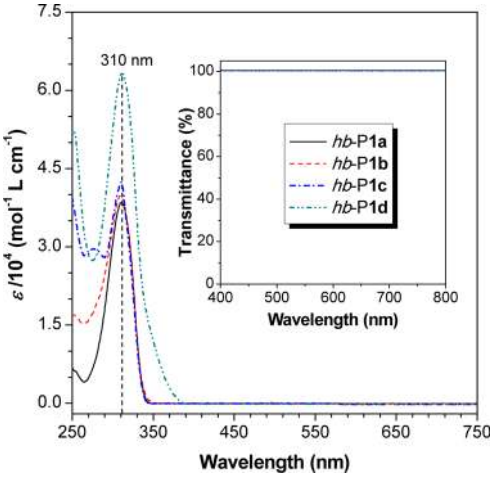

Figure 5. UV spectra of *hb*-P**1a**–**d** in THF solutions. Solution concentration: 10^{-5} M. Inset: transmission spectra of *hb*-P**1a**–**d** in THF solutions at wavelengths from 400 to 800 nm.

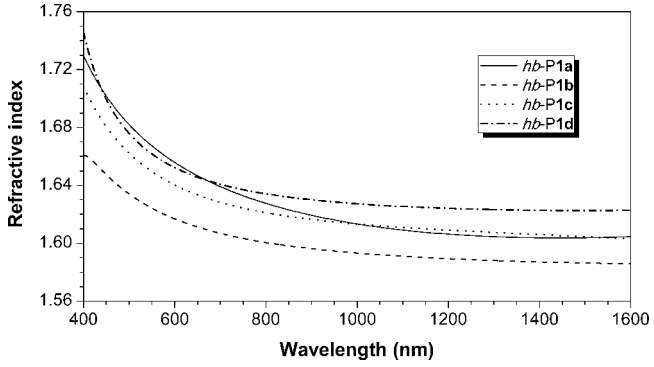

Figure 7. Wavelength dependence of refractive index of thin films of *hb*-P**1a**–**d**.

polymers at 633 nm are 1.6496, 1.6130, 1.6356 and 1.6477, which are much higher than those of the commercially important optical plastics, such as polystyrene (n = 1.59), poly(methyl methacrylate) (n = 1.49) and polycarbonate (n = 1.59).[26] Little birefringence is detected, indicating the amorphous nature of their thin solid films.

Chromatic Dispersion. Abbé number is a measure of the dispersion of the materials in relation to the refractive index and a key parameter for optical materials used in the visible region.

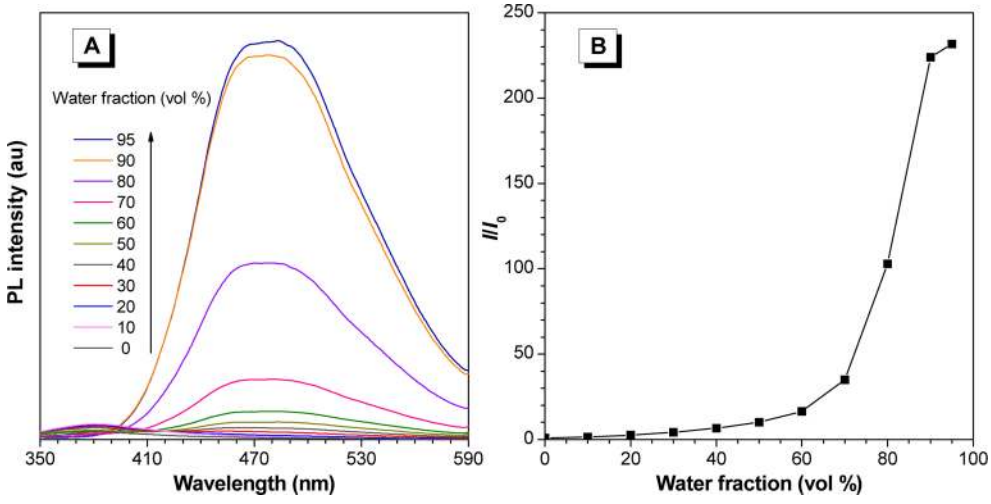

Figure 6. (A) PL spectra of *hb*-P**1d** in THF and THF/H_2O mixtures. Concentration: 10^{-5} M; excitation wavelength: 310 nm. (B) Plot of I/I_0 values versus the compositions of the THF/H_2O mixtures of *hb*-P**1d**.

dx.doi.org/10.1021/ma402066k | *Macromolecules* 2013, 46, 9494–9506

Table 7. Refractive Indices and Chromatic Dispersions of *hb*-P1a−d[a]

polymer	n_{633}	n_{1550}	Δn_{633}	ν_D	ν_D'	D	D'
hb-P**1a**	1.6496	1.6039	0.007	15.9	95.6	0.063	0.010
hb-P**1b**	1.6130	1.5860	0.001	23.1	102.7	0.043	0.010
hb-P**1c**	1.6356	1.6038	0.001	18.9	76.5	0.053	0.013
hb-P**1d**	1.6477	1.6227	0.003	18.0	187.4	0.056	0.005

[a]Abbreviation: n = refractive index, Δn = birefringence, ν_D = Abbé number = $(n_D-1)/(n_F-n_C)$, where n_D, n_F and n_C are the RI values at wavelengths of 589.2, 486.1, and 656.3 nm, respectively, ν_D' = modified Abbé number = $(n_{1319}-1)/(n_{1064}-n_{1550})$, where n_{1319}, n_{1064} and n_{1550} are the RI values at 1319, 1064, and 1550 nm, respectively, $D^{(\prime)}$ = chromatic dispersion $=1/\nu_D^{(\prime)}$.

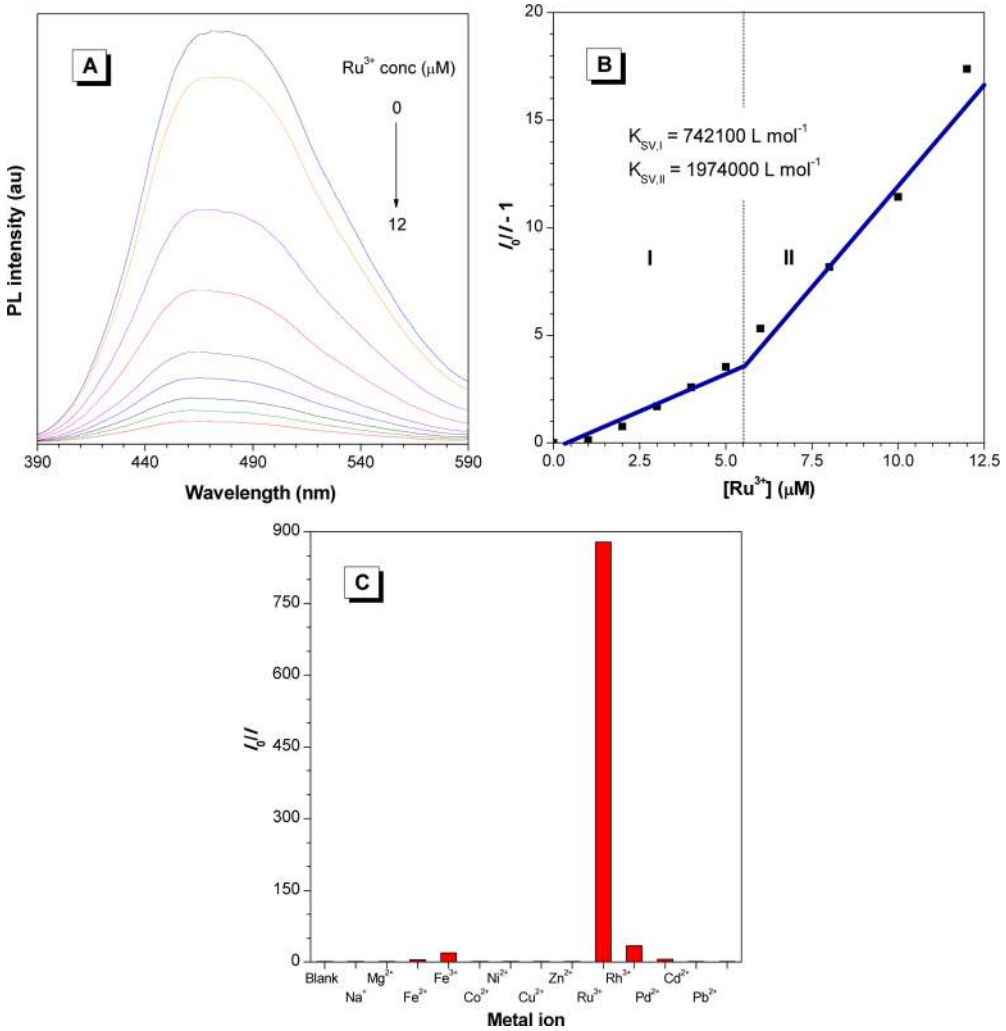

Figure 8. (A) PL spectra of *hb*-P**1d** in THF/H_2O mixtures (1:9 by volume; 10 μM) with various Ru^{3+} concentrations. (B) Stern−Volmer plot of $(I_0/I-1)$ values versus Ru^{3+} concentrations in THF/H_2O mixtures (1:9 by volume) of *hb*-P**1d**. I_0 = intensity in the absence of metal ions. (C) Selectivity of *hb*-P**1d** toward different metal ions.

It is defined as: $\nu_D = (n_D - 1)/(n_F - n_C)$, where n_D, n_F and n_C are the RI values at Fraunhofer D, F, and C spectral lines of 589.3, 486.1, and 656.3 nm, respectively.[27] A modified Abbé number (ν_D') is proposed to evaluate the application potential of an optical material using its RI values at the nonabsorbing infrared wavelengths of 1064, 1319, and 1550 nm. The modified Abbé number is defined as: $\nu_D' = (n_{1319} - 1)/(n_{1064} - n_{1550})$, where n_{1319}, n_{1064}, and n_{1550} are the RI values at 1319, 1064, and 1550 nm, respectively. The chromatic dispersions (D and D') in the visible and infrared regions are the reciprocals of ν_D and ν_D' and defined as $D^{(\prime)} = 1/\nu_D^{(\prime)}$.

The ν_D and ν_D' values of *hb*-P**1a−d** are in the range of 15.9−23.1 and 76.5−187.4, corresponding to D and D' values of 0.043−0.063 and 0.005−0.013, respectively (Table 7). These values suggest that *hb*-P**1a−d** possess low spectral aberrations. Together with their high optical transparencies and light refractivities, the present polymers are anticipated to be promising coating materials used in advanced optical display systems.

Metal-Ion Detection. Ruthenium(III) ion is the most commonly available ruthenium compound and works as a precursor to many chemical compounds. They are corrosive and destructive to the respiratory tract, eyes, skin, and digestive tract once contact with them. Thus, sensitive, reliable, and practicable methods are required for its detection at trace level. Among various analytical techniques, fluorescence stands out

dx.doi.org/10.1021/ma402066k | *Macromolecules* 2013, 46, 9494−9506

due to its high sensitivity. Polytriazine *hb*-P**1d** shows AIE characteristic and consists of chelating triazine rings, and thus it may serve as a sensitive and selective fluorescent chemosensor for Ru^{3+} ion detection.

Gradual addition of Ru^{3+} ion to the nanoparticle suspension of *hb*-P**1d** in THF/H_2O mixture (1:9 by volume) decreases its emission progressively (Figure 8A). The PL quenching can be clearly recognized at a low Ru^{3+} concentration of 1 μg mL^{-1}. At $[Ru^{3+}]$ = 12 μM, the PL of the polymer is almost quenched completely. The PL annihilation may be attributed to the electrostatic interaction between the electron-rich TPE unit and the electron-deficient Ru^{3+} ion and the chelation of triazine ring with the metal ion. The Stern−Volmer plot of $(I_0/I-1)$ values versus Ru^{3+} concentrations for the nanoaggregates of *hb*-P**1d** suspended in the aqueous mixture is shown in Figure 8B. Bending-upward curves, instead of straight line, was obtained, indicating that the PL quenching becomes more efficient with increasing quencher concentration. The Stern−Volmer constant (K_{sv}) or the quenching efficiency can be determined from the Stern−Volmer plot. Interestingly, the plot is composed of two stages. In stage I or in the low Ru^{3+} concentration ($\leq$5.0 μM), the plot is linear with a $K_{SV,I}$ value of 742100 L mol^{-1}. When the Ru^{3+} concentration is increased to >5.0 μM or in the high quencher concentration region, the Stern−Volmer plot is deviated from the linear one for the low $[Ru^{3+}]$ region and enters stage II, where the plot follows another linear relationship with a 2.7-fold higher quenching efficiency ($K_{SV,II}$ = 1974000 L mol^{-1}). This reveals a superamplification effect in the emission quenching process. The nanoaggregates of *hb*-P**1d** possess a large number of cavities to bind with many quencher molecules and many interchain diffusion pathways for excitons to migrate, thus making the quenching a highly efficient process.

To evaluate whether the Ru^{3+} detection is selective, we studied the PL change of the polymer in the presence of other metal ions. As shown in Figure 8C, addition of other metal ions, including Na^+, Mg^{2+}, Fe^{2+}, Fe^{3+}, Co^{2+}, Ni^{2+}, Cu^{2+}, Zn^{2+}, Rh^{3+}, Pd^{2+}, Cd^{2+} and Pb^{2+} exerts little change on the PL spectrum of *hb*-P**1d**, which is indicative of its high selectivity toward Ru^{3+}. Although the reason for such selectivity remains unclear at present, we believe that the higher standard reduction potential of the Ru(III)/Ru(0) couple relative to other cation/metal systems may be responsible for such selective sensing.

CONCLUSIONS

In this work, we developed a new polymerization route for the synthesis of heteroatom-containing hyperbranched polymers. Instead of using alkyne monomers, we explored the possibility of utilizing nitriles as building blocks. The polycyclotrimerization of dinitriles **1a−d** proceeds smoothly in the presence of trifluoromethanesulfonic acid at room temperature in *o*-DCB, producing nitrogen-rich polytriazines *hb*-P**1a−d** with high DB in high isolated yields. Model reaction was performed to assist structural characterization of the polymers. The resulting polymers are processable and optically transparent. They enjoy high thermal and morphological stabilities. Their films exhibit high refractive indices and low chromatic aberrations. Polymerization of TPE-containing dinitrile generates a polymer with AIE characteristic, enabling it to be utilized as a sensitive and selective fluorescent chemosenor for ruthenium(III) ion detection.

AUTHOR INFORMATION

Corresponding Author

*E-mail: tangbenz@ust.hk. Phone: +852-2358-7375. Fax: +852-2358-1594.

Notes

The authors declare no competing financial interest.

ACKNOWLEDGMENTS

The present work was partially supported by the National Basic Research Program of China (973 Program; 2013CB834701), the Research Grants Council of Hong Kong (604913, 604711, 602212, HKUST2/CRF/10 and N_HKUST620/11) and the University Grants Committee of Hong Kong (AoE/P-03/08). B.Z.T. thanks the support of the Guangdong Innovative Research Team Program (201101C0105067115).

REFERENCES

(1) (a) Yan, D.; Gao, C.; Frey, H. *Hyperbranched Polymers: Synthesis, Properties, and Applications*; John Wiley & Sons, Inc.: Hoboken, NJ, 2011. (b) Jikei, M.; Kakimoto, M. *Prog. Polym. Sci.* **2001**, *26*, 1233−1285. (c) Voit, B. *J. Polym. Sci., Part A: Polym. Chem.* **2000**, *38*, 2505−2525. (d) Froehling, P. *J. Polym. Sci., Part A: Polym. Chem.* **2004**, *42*, 3110−3115. (e) Gao, C.; Yan, D. *Prog. Polym. Sci.* **2004**, *29*, 183−275. (f) Voit, B. *J. Polym. Sci., Part A: Polym. Chem.* **2005**, *43*, 2679−2699.

(2) (a) Frechet, J. M. J.; Henmi, M.; Gitsov, I.; Aoshima, S.; Leduc, M. R.; Grubbs, R. B. *Science* **1995**, *269*, 1080−1083. (b) Hawker, C. J.; Frechet, J. M. J.; Grubbs, R. B.; Dao, J. *J. Am. Chem. Soc.* **1995**, *117*, 10763−10764. (c) Gaynor, S. G.; Edelman, S.; Matyjaszewski, K. *Macromolecules* **1996**, *29*, 1079−1081. (d) Suzuki, M.; Yobbshida, S.; Shiraga, K.; Saegusa, T. *Macromolecules* **1998**, *31*, 1716−1719. (e) Sunder, A.; Hanselmann, R.; Frey, H.; Muelhaupt, R. *Macromolecules* **1999**, *32*, 4240−4246.

(3) (a) Yan, D.; Zhou, Z.; Mueller, A. H. E. *Macromolecules* **1999**, *32*, 245−250. (b) Cheng, C.; Wooley, K. L.; Khoshdel, E. *J. Polym. Sci., Part A: Polym. Chem.* **2005**, *43*, 4754−4770. (c) Simon, P. F. W.; Radke, W.; Muller, A. H. E. *Macromol. Rapid Commun.* **1997**, *18*, 865−873. (d) Matyjaszewski, K.; Gaynor, S. G.; Kulfan, A.; Podwika, M. *Macromolecules* **1997**, *30*, 5192−5194. (e) Baskaran, D. *Polymer* **2003**, *44*, 2213−2220.

(4) For reviews: (a) Hu, R.; Lam, J. W. Y.; Tang, B. Z. *Macromol. Chem. Phys.* **2013**, *214*, 175−187. (b) Qin, A.; Lam, J. W. Y.; Tang, B. Z. *Prog. Polym. Sci.* **2012**, *37*, 182−209. (c) Qin, A.; Lam, J. W. Y.; Tang, B. Z. *Macromolecules* **2010**, *43*, 8693−8702. (d) Qin, A.; Lam, J. W. Y.; Tang, B. Z. *Chem. Soc. Rev.* **2012**, *39*, 2522−2544. (e) Liu, J.; Lam, J. W. Y.; Tang, B. Z. *Chem. Rev.* **2009**, *109*, 5799−5867. (f) Lam, J. W. Y.; Tang, B. Z. *Acc. Chem. Res.* **2005**, *38*, 745−754.

(5) (a) Häußler, M.; Tang, B. Z. *Adv. Polym. Sci.* **2007**, *209*, 1−58. (b) Häußler, M.; Qin, A.; Tang, B. Z. *Polymer* **2007**, *48*, 24−25. (c) Häußler, M.; Lam, J. W. Y.; Zheng, R.; Peng, H.; Luo, J.; Chen, J.; Law, C. C. W.; Tang, B. Z. *C. R. Chim.* **2003**, *6*, 833−842. (d) Dong, H.; Lam, J. W. Y.; Häußler, M.; Zheng, R.; Peng, H.; Law, C. C. W.; Tang, B. Z. *Curr. Trends Polym. Sci.* **2004**, *9*, 15−31.

(6) (a) Liu, J.; Zheng, R.; Tang, Y.; Häußler, M.; Lam, J. W. Y.; Qin, A.; Ye, M.; Hong, Y.; Gao, P.; Tang, B. Z. *Macromolecules* **2007**, *40*, 7473−7486. (b) Häußler, M.; Liu, J.; Zheng, R.; Lam, J. W. Y.; Qin, A.; Tang, B. Z. *Macromolecules* **2007**, *40*, 1914−1925. (c) Zheng, R.; Häußler, M.; Dong, H.; Lam, J. W. Y.; Tang, B. Z. *Macromolecules* **2006**, *39*, 7973−7984. (d) Li, Z.; Lam, J. W. Y.; Dong, Y. Q.; Dong, Y. P.; Sung, H. H. Y.; Williams, I. D.; Tang, B. Z. *Macromolecules* **2006**, *39*, 6458−6466. (e) Li, Z.; Qin, A.; Lam, J. W. Y.; Dong, Y. Q.; Dong, Y. P.; Ye, C.; Williams, I. D.; Tang, B. Z. *Macromolecules* **2006**, *39*, 1436−1442.

(7) (a) Jim, C. K. W.; Qin, A.; Lam, J. W. Y.; Häussler, M.; Liu, J.; Yuen, M. M. F.; Kim, J. K.; Ng, K. M.; Tang, B. Z. *Macromolecules* **2009**, *42*, 4099−4109. (b) Qin, A.; Lam, J. W. Y.; Dong, H.; Lu, W.; Jim, C. K. W.; Dong, Y. Q.; Häußler, M.; Sung, H. H. Y.; Williams, I. D.; Wong, G. K. L.; Tang, B. Z. *Macromolecules* **2007**, *40*, 4879−4886.

(c) Dong, H.; Zheng, R.; Lam, J. W. Y.; Häußler, M.; Tang, B. Z. *Macromolecules* **2005**, *38*, 6382−6391.
(8) Liu, J.; Zhang, L.; Lam, J. W. Y.; Jim, C. K. W.; Yue, Y.; Deng, R.; Hong, Y.; Qin, A.; Sung, H. H. Y.; Williams, I. D.; Jia, G.; Tang, B. Z. *Macromolecules* **2009**, *42*, 7367−7378.
(9) (a) Acheson, R. M. *An Introduction to the Chemistry of Heterocyclic Compounds*, 2nd ed.; Wiley: New York, 1967. (b) Gilchrist, T. L. *Heterocyclic Chemistry*, 2nd ed.; Longman: Harlow, U.K., 1992.
(10) (a) Jonkhejim, P.; Miura, A.; Zdanowska, M. F.; Hoeben, J. M.; DeFeyter, S.; Schenning, A. P. H. J.; De Schryver, F. C.; Meijer, E. W. *Angew. Chem., Int. Ed.* **2004**, *43*, 74−78. (b) Malek, N.; Maris, T.; Simard, M.; Wuest, J. D. *J. Am. Chem. Soc.* **2005**, *127*, 5910−5916. (c) Ranganathan, A.; Pedireddi, V. R.; Rao, C. N. R. *J. Am. Chem. Soc.* **1999**, *121*, 1752−1753.
(11) (a) Robson, R. *J. Chem. Soc., Dalton Trans.* **2000**, 3735−3744. (b) Fujita, M.; Tominaga, M.; Hori, A.; Therrien, B. *Acc. Chem. Res.* **2005**, *38*, 371−380. (c) Maurizot, V.; Yoshizawa, M.; Kawano, M.; Fujita, M. *Dalton Trans.* **2006**, 2750−2756. (d) Kobayashi, Y.; Kawano, M.; Fujita, M. *Chem. Commun.* **2006**, 4377−4379.
(12) (a) Luo, H. M.; Wang, H.; Zeng, Z.; Zeng, H. P. *Chin. J. Org. Chem.* **2013**, *33*, 915−926. (b) Wang, D. X.; Li, B.; Zhang, Y. H.; Lu, Z. J. *J. Appl. Polym. Sci.* **2013**, *127*, 516−522. (c) Dominguez, G.; Perez-Castells, J. *Chem. Soc. Rev.* **2011**, *40*, 3430−3444. (d) Deng, Z. X.; Qin, W. F.; Li, W. J. *Chin. Sci. Bull.* **2004**, *48*, 127−130. (e) Fan, X.; Zhu, X. H.; Shen, Q.; Jun, L.; Li, J. Q. *Chin. J. Chem.* **2002**, *20*, 1334−1339. (f) Tao, X. C.; Tao, H.; Liu, T. P.; Qian, Y. L. *Chin. J. Catal.* **2002**, *23*, 99−100. (g) Diaz-Ortiz, A.; de la Hoz, A.; Moreeno, A.; Sanchez-Migallon, A.; Valiente, G. *Green. Chem.* **2002**, *4*, 339−343. (h) Xu, F.; Sun, J. H.; Yan, H. B.; Shen, Q. *Synth. Commun.* **2000**, *30*, 1017−1022. (i) Zhang, W. M.; Liao, S. J.; Xu, Y.; Zhang, Y. P. *Synthet. Commun.* **1997**, *27*, 3977−3983. (j) Armstrong, D. R.; Henderson, K. W.; Macgregor, M.; Mulvey, R. E.; Ross, M. J.; Clegg, W.; Oneil, P. A. *J. Organomet. Chem.* **1995**, *486*, 79−83. (k) Lopez, G.; Sanchez, G.; Garcia, G.; Ruiz, J.; Garcia, J.; Martinezripoll, M.; Vegas, A.; Hermoso, J. A. *Angew. Chem., Int. Ed.* **1991**, *30*, 716−717. (l) Koppes, W. H.; Adolph, H. G. *J. Org. Chem.* **1981**, *46*, 406−412.
(13) Norell, J. R. US Patent No. 3 932 402, 1976.
(14) Chen, X.; Bai, S. D.; Wang, L.; Liu, D. S. *Heterocycles* **2005**, *65*, 1425−1430.
(15) (a) Kuhn, P.; Antonietti, M.; Thomas, A. *Angew. Chem., Int. Ed.* **2008**, *47*, 3450−3453. (b) Bojdys, M. J.; Jeromenok, J.; Thomas, A.; Antonietti, M. *Adv. Mater.* **2010**, *22*, 2202−2205. (c) Kuhn, P.; Forget, A.; Su, D.; Thomas, A.; Antonietti, M. *J. Am. Chem. Soc.* **2008**, *130*, 13333−13337. (d) Ren, S.; Bojdys, M. J.; Dawson, R.; Laybourn, A.; Khimyak, Y. Z.; Adams, D. J.; Cooper, A. I. *Adv. Mater.* **2012**, *24*, 2357−2361.
(16) (a) Muchtar, Z.; Schappacher, M.; Deffieux, A. *Macromolecules* **2001**, *34*, 7595−7600. (b) Uhrich, K. E.; Hawker, C. J.; Frechet, J. M. J.; Turner, S. R. *Macromolecules* **1992**, *25*, 4583−4587.
(17) Zheng, R. H.; Dong, H. C.; Peng, H.; Lam, J. W. Y.; Tang, B. Z. *Macromolecules* **2004**, *37*, 5196−5210. (b) Peng, H.; Cheng, L.; Luo, J.; Xu, K.; Sun, Q.; Dong, Y.; Salhi, F.; Lee, P. P. S.; Chen, J.; Tang, B. Z. *Macromolecules* **2002**, *35*, 5349−5351.
(18) (a) Voit, B. I.; Lederer, A. *Chem. Rev.* **2009**, *109*, 5924−5973. (b) Gao, C.; Yan, D. *Prog. Polym. Sci.* **2004**, *29*, 183−275. (c) Kim, Y. *J. Polym. Sci., Part A: Polym. Chem.* **1998**, *36*, 1685−1698.
(19) (a) Young, R. J.; Lovell, P. A. *Introduction to Polymers*, 2nd ed., Champman & Hall: London, 1991. (b) Hawker, C. J.; Lee, R.; Frechet, J. M. J. *J. Am. Chem. Soc.* **1991**, *113*, 4583−4588. (c) Frey, H.; Holter, D. *Acta Polym.* **1999**, *50*, 67−76.
(20) (a) Yan, D. Y.; Muller, A. H. E.; Matyjaszewski, K. *Macromolecules* **1997**, *30*, 7024−7033. (b) Ishizu, K.; Tsubaki, K.; Mori, A.; Uchida, S. *Prog. Polym.* **2003**, *28*, 27−54. (c) Grebel-Koehler, D.; Liu, D. J.; De Feyter, S.; Enkelmann, V.; Weil, T.; Engels, C.; Samyn, C.; Muller, K.; De Schryver, F. C. *Macromolecules* **2003**, *36*, 578−590.
(21) Luo, J.; Xie, Z.; Lam, J. W. Y.; Cheng, L.; Chen, H. Y.; Qiu, C. F.; Kwok, H. S.; Zhan, X. W.; Liu, Y. Q.; Zhu, D. B.; Tang, B. Z. *Chem. Commun.* **2001**, 1740−1741.
(22) For reviews, see: (a) Hong, Y.; Lam, J. W. Y.; Tang, B. Z. *Chem. Soc. Rev.* **2011**, *40*, 5361−5388. (b) Hong, Y.; Lam, J. W. Y.; Tang, B. Z. *Chem. Commun.* **2009**, 4332−4353. (c) Liu, J.; Lam, J. W. Y.; Tang, B. Z. *J. Inorg. Organomet. Polym. Mater.* **2009**, *19*, 249−285.
(23) Birks, J. B. *Photophysics of Aromatic Molecules*; Wiley: London, 1970.
(24) (a) Hu, R.; Maldonado, J. L.; Rodriguez, M.; Deng, C.; Jim, C. K. W.; Lam, J. W. Y.; Yuen, M. M. F.; Ramos-Ortiz, G.; Tang, B. Z. *J. Mater. Chem.* **2012**, *22*, 232−240. (b) Liu, J.; Zhong, Y.; Lam, J. W. Y.; Lu, P.; Hong, Y.; Yu, Y.; Yue, Y.; Mahtab, F.; Sung, H. H. Y.; Williams, I. D.; Wong, K. S.; Tang, B. Z. *Macromolecules* **2010**, *43*, 4921−4936. (c) Kokado, K.; Chujo, Y. *Macromolecules* **2009**, *42*, 1418−1420. (d) Liu, J.; Zhong, Y.; Lu, P.; Hong, Y.; Lam, J. W. Y.; Mahtab, F.; Yu, Y.; Wong, K. S.; Tang, B. Z. *Polym. Chem.* **2010**, *1*, 426−429. (e) Qin, A.; Jim, C. K. W.; Tang, Y. H.; Lam, J. W. Y.; Liu, J.; Mahtab, F.; Gao, P.; Tang, B. Z. *J. Phys. Chem. B* **2008**, *112*, 9281−9288.
(25) (a) Gao, C.; Yang, B.; Shen, J. *J. Appl. Polym. Sci.* **2000**, *75*, 1474−1479. (b) Matsuda, T.; Funae, Y.; Yoshida, M.; Yamamoto, T.; Takaya, T. *J. Appl. Polym. Sci.* **2000**, *76*, 45−49.
(26) (a) Seferis, J. C. *Polymer Handbook*, 3rd ed.; Brandrup, J.; Immergut, E. H., Eds., Wiley: New York, 1989; pp VI/451−VI/461. (b) Mills, N. J. *Concise Encyclopedia of Polymer Science & Engineering*; Kroschwitz, J. I., Ed.; Wiley: New York, 1990; pp 683−687.
(27) Hecht, E. *Optics*, 4th ed.; Addison Wesley: San Francisco, CA, 2002.